

Age of Information and Energy Consumption in IoT: an Experimental Evaluation

Federico Cristofani
University of Pisa, Italy
f.cristofani@studenti.unipi.it

Valerio Luconi
IIT-CNR, Italy
valerio.luconi@iit.cnr.it

Alessio Vecchio
University of Pisa, Italy
alessio.vecchio@unipi.it

Abstract—The Age of Information (AoI) is an end-to-end metric frequently used to understand how “fresh” the information about a remote system is. In this paper, we present an experimental study of the relationship between AoI and the energy spent by the device that produces information, e.g. an IoT device or a monitoring sensor. Such a relationship has been almost neglected so far, but it is particularly important whenever the sensing side is battery-operated. The study is carried out in a scenario where access is achieved via the cellular network and information is transferred using MQTT, a popular messaging protocol in the IoT domain. Numerous parameters of operation are considered, and the most efficient solutions in all configurations are provided.

Index Terms—Age of Information, energy, Internet of Things, QUIC, TCP, MQTT

I. INTRODUCTION

Age of Information (AoI) has emerged as a critical metric reflecting the timeliness and relevance of data delivery. In a monitoring system, AoI is defined as the time elapsed since the generation of the latest received packet at the monitor, and it can capture the freshness of the received data better than classic metrics such as delay [1]. In today’s interconnected world, where real-time data processing and transmission are paramount, understanding and optimizing the AoI is pivotal for a spectrum of applications, including multimedia streaming, Internet of Things (IoT) deployments, and financial transactions. Since its introduction [2], AoI has been used as a metric to analyze and characterize a wide variety of systems, especially IoT-related such as intelligent transportation systems, vehicular networks, smart agriculture, and augmented reality [3]–[5].

Alongside the quest for timely information delivery, the energy footprint of network protocols and infrastructure has gained significant attention. With the exponential growth of digital traffic, data centers, and communication networks, the environmental impact of energy-intensive operations has become a focal point for researchers, policymakers, and industry stakeholders alike. Especially in the IoT context, energy consumption considerations gain paramount importance, since most of the devices are battery-operated [6]–[9].

Recently, various studies have investigated the trade-off between maintaining a desired freshness level of information while minimizing energy consumption in IoT systems, mainly from a theoretical perspective [10], [11]. Conversely, recent experimental works still have not focused on the implication

of AoI on energy but were mainly aimed at studying AoI-aware systems in some operating scenarios [12], [13].

In this work, we aim to evaluate the relationship between AoI and energy consumption in an experimental publish-subscribe scenario. We built a testbed made of an IoT device that publishes updates at a given rate, and we measure AoI at a subscriber. Simultaneously, we measure energy consumption via a hardware power monitor on the IoT device. The devices are connected via a cellular network and communicate through the MQTT protocol on top of QUIC and TLS. We run an extensive set of experiments to explore how a wide range of parameters of operations can influence the two considered metrics. In detail, we considered the rate of generation of messages on the IoT device, the latency between the IoT device and the MQTT broker, the messages’ payload size, the computational capacity of the IoT device, and the impact of the underlying transport protocol. Thanks to the visualization instrument of Pareto fronts, we point out the most efficient solutions for every configuration of parameters. We show that there is no clear indication of a universally optimal solution, but the context and the system’s requirements should indicate which of the most efficient solutions to adopt. However, we believe that our experimental results are extremely precious in helping researchers and practitioners in future protocol designs, IoT system architectures, and environmental sustainability initiatives.

The rest of the paper is structured as follows. Section II provides an overview of the existing literature on the subject. Section III describes our experimental setup. In Section IV, we describe the metrics and the aggregation techniques that we use to analyze experimental results. Section V shows our findings. Finally, Section VI concludes the paper.

II. RELATED WORK

The performance of transport and application protocols in an IoT context has been extensively studied from various points of view. Several works have evaluated the adoption of the recently introduced QUIC transport protocol in IoT. In [14] the authors demonstrated the feasibility of a QUIC standard implementation designed for tiny devices, by quantifying storage, computing, memory, and energy requirements, however, without involving any application protocol. Other studies have used HTTP as an application protocol over QUIC in an IoT environment. In [15], the authors studied the latency

and scalability of HTTP/3 over QUIC in an IoT system in the cloud/edge continuum, showing results in the order of hundreds or thousands of milliseconds depending on the load of the system. The energetic performance of HTTP protocols have been studied for both IoT devices and smartphones in [8], [9], where the authors compared different versions of the HTTP, showing that the ones using QUIC as an underlying protocol consumed more energy. The authors also showed that their results could be due to the current lack of maturity and standardized adoption of QUIC implementations, among other factors. Fatima et al. compared QUIC and TCP/TLS as underlying protocols of MQTT, for what concerns latency, in a simulated environment. They showed that, for short-lived connections, the performance of the two protocols is comparable, while for long-lived connections, QUIC obtains shorter completion times. The same comparison is conducted in [16] for a IIoT-cloud environment based on MQTT. Again, QUIC obtained a much better performance. In [17], the authors analyzed MQTT over QUIC and TCP/TLS from the energetic point of view, showing that for small-medium delays QUIC was able to consume less energy, while for large ones TCP/TLS obtained a slightly better performance.

Work on AoI focused on theoretically analyzing the performance of different systems characterized by different queuing models and scheduling algorithms in different application scenarios [18]–[21].

The relationship between energy and AoI has been investigated mainly from a theoretical point of view. In [10], the authors devise two scheduling algorithms for multiple sensors that minimize the AoI at the monitoring station. Subsequently, energy consumption is brought into play and the authors show variants to their algorithms that can achieve close to optimal performance with significant energy consumption reduction. A framing and scheduling policy for minimizing energy consumption in cognitive wireless sensor networks has been proposed in [11]. The optimization is conducted under strict constraints of AoI. Via numerical and simulation analysis, the authors provide the optimal number of samples per packet under given operational conditions, such as the number of nodes in the network and channel quality indicators. In [22], the authors derive closed forms for AoI and energy consumption in an IoT monitoring system based on low power wide area (LPWA) wireless communication technologies and adopting a truncated automatic repeat request (TARQ) scheme. The authors show that under transmit power constraint, the TARQ scheme obtains lower AoI than a classic ARQ scheme. The problem of minimizing energy consumption under AoI constraints has been studied also in [23], where the authors derived a lower bound on the competitive ratio of any given causal policy for choosing which packets to transmit on a given node. In addition, they propose a greedy policy that achieves that lower bound. Other works have tackled the problem of AoI and energy from different perspectives, for example for an energy harvesting source [24], or computation offloading in industrial IoT [25].

Few works focused on evaluating AoI in experimental

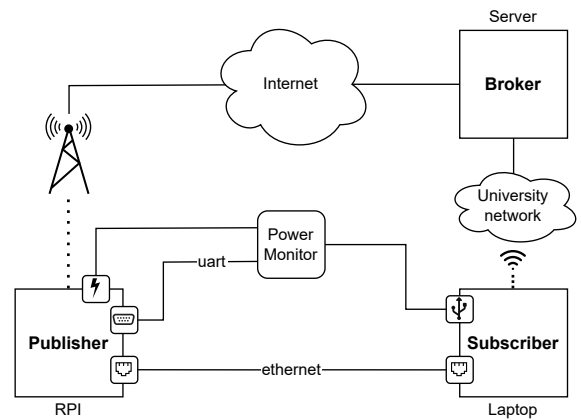


Fig. 1: Experimental setup hardware and software architecture.

environments. In [26], the AoI of a TCP/IP connection over WiFi, Ethernet, and cellular networks has been investigated via emulation and in a physical network. Observations have been conducted with different sampling rates and degree of network load. The AoI of TCP and UDP connections over the Internet and of lightweight IoT connections in a local WiFi network has been evaluated in [12]. In this work, the authors provide insight into how energy can be a factor impacting AoI in constrained environments such as IoT. In [13], the authors proposed WiFresh: an AoI-aware wireless architecture to achieve optimal AoI even in the case of an overloaded network. They show that compared to classic WiFi, WiFresh can obtain lower values of AoI.

The analysis of the previous works reveals considerable attention to topics related to the IoT, highlighting extensive coverage of these issues. In particular, the emerging protocol as QUIC is gaining popularity as a modern alternative to the de-facto standard TCP that showed limitations for lossy networks and constrained devices. The focus is also placed on the AoI metric, able to represent the freshness of data, that in modern systems assumes a pivotal role. However, significant gaps emerged. Among all, there is a lack of experimental works, especially regarding combined studies on AoI and energy. This work is placed at the intersection of studies exploring energy consumption and AoI in IoT, adopting an experimental methodology. To the best of our knowledge, ours is the first experimental work that analyzes AoI and energy consumption in a real-world IoT scenario.

III. EXPERIMENTAL SETUP

This study aims to evaluate Age of Information (AoI) and the energy consumption in a IoT scenario, using the MQTT protocol running on top of multiple transport protocols: QUIC and TCP/TLS. We built the experimental setup depicted in Figure 1, composed of multiple hardware and software components. The RPI acts as an IoT device, hosting the client side, i.e. the publisher in the MQTT terminology. The RPI is equipped with a cellular network card [27] able to support both Long Term Evolution (LTE 4G) and New Generation (NG 5G)

TABLE I: Experimental setup hardware specs.

Device	CPU	RAM	NIC
RPI	BCM2837B0 ARMv8 64bit ¹	1GB LPDDR2	SIM8200EA-M2 5G HAT
Laptop	Intel Core i7-8565U	16GB DDR4	Intel(R) Wireless-AC 9260
Server	Intel Xeon Gold 5120 ²	4GB	Ethernet adapter

Ethernet interfaces for RPI and the laptop are not reported in the table

TABLE II: Network connections in the experimental setup.

Connection	RTT	Download	Upload	Hops
RPI - Server	80 ms	28 Mbit/s	15 Mbit/s	12
Laptop - Server	5 ms	200 Mbit/s	160 Mbit/s	3

communication technologies³. The RPI represents a battery-powered device. To measure its power consumption, it is powered by the Otii Arc Pro from Qoitech power monitor [28]. The Otii power monitor is featured with a Asynchronous Receiver-Transmitter (UART) interface that is used to send commands to the RPI device and to annotate the recorded trace with timestamps to precisely confine the portion of the total energy required during the execution of an experiment. The RPI publisher is then connected via cellular connection to a MQTT broker hosted on a server in the University of Pisa cloud network.

The final component of the experimental setup is a laptop, which has a twofold function. Firstly, it acts as a MQTT subscriber client, connected to the broker via the University of Pisa network (with WiFi access). The connection between the broker and the subscriber is characterized by a relatively low latency, being the two components in the same network. Secondly, the laptop acts as the controller of the experiments. It is connected to both the RPI and the Otii to provide the configuration parameters and the automation for each experiment.

The goal of the study is to evaluate the system from the point of view of the AoI and the energy needed on the publisher side. We are not interested in the energy consumption of the machine hosting the subscriber as we suppose that the alerting/controlling system mentioned before is not executed on a battery-operated device. Similarly, the energy needed to run the broker is not of interest, as it is generally executed on reasonably powerful machines without constraints in terms of energy. With this setup, we can measure both the energy consumption on the RPI and the AoI, as the difference between the instant when the message was generated and the instant when it was received. To obtain a precise measure of the AoI, the two devices (the Raspberry Pi 3B+ and the laptop) need to be adequately synchronized. To achieve the desired synchronization, we used an approach based on the Network Time Protocol (NTP) protocol. The two devices are connected via a second ethernet connection, and the laptop

acts as the time-reference server for the RPI. The ethernet connection is characterized by an extremely low latency, being the two devices in the same lab room, and is used only for synchronization traffic. All the other traffic exchanged by the two devices flows via the cellular connection and the Internet.

The overall configuration corresponds to a rather common scenario in the IoT domain, in which the RPI acts as a device installed somewhere that produces data, typically collecting information by monitoring the environment. The subscriber on the laptop in turn can be considered as a cloud application that deals with the collection of the data produced, applying logic that may be sensitive to the freshness of the information obtained from the data. The two parties exchange information through the broker, hosted in the cloud as the subscriber, which represents a centralized entity enabling indirect communication according to the MQTT protocol. Table I summarizes the hardware specs of the experimental setup, while Table II provides a characterization of the network connections between the hardware components.

A. Implementation

The client has been implemented relying on the Quinn library [29], a rust-based implementation of the IETF QUIC protocol. We did not use a standard MQTT client as available QUIC-based implementations are rather limited in number. Quinn provides an async API and it is based on the Tokio async runtime [30]. Quinn also uses the Rustls [31] library for the cryptographic functionality. In particular, our client also uses the mqttbytes [32] libraries for producing MQTT messages according to the specification. The client just implements the subset of the MQTT protocol needed for our experiments, like sending messages to the broker and receiving the corresponding acknowledgments. To achieve higher message rates, the client uses a task to send messages to the broker and another task to keep track of the corresponding incoming acks. The client also includes the buffering mechanisms previously mentioned: a task produces new information at a nominal rate and uses a buffer to communicate with the sender task. The latter is responsible for extracting information from the buffer and sending it through the network. The buffer is managed according to two strategies: (i) a FIFO queue with a capacity of 1, 16, and 1024 messages, and (ii) a drop-head-on-full queue of capacity 1. In the first case, the two tasks can be blocked when the queue is full or empty and no messages are lost. In the second case, a message can be lost if a new one is produced before the current one is transmitted. In this case, the producing task never blocks and always operates

³Experiments have been carried out only using 4G access.

according to the nominal rate. The strategies will be hereafter indicated as FIFO 1, FIFO 16, FIFO 1024, and DROP. The broker is an instance of the Rumqtt server. The subscriber is rather simple and receives messages when relayed by the broker. The subscriber computes the AoI, by using a timestamp collected when the message is received and another timestamp included in the message by the publisher and indicating the time when the message was produced. The subscriber has been implemented using the Paho library [33].

IV. COLLECTED METRICS AND AGGREGATION

To make the paper self-contained, we here provide a description of the metrics and the aggregation tools that we consider in this study.

A. Age of Information

The recording of generation and reception instants of the message published during the time window gives all the information needed to compute the AoI not only in correspondence with the message arrival but in any instant along the entire duration of the experiment, obtaining an exact form for the sawtooth shape function that characterizes the metric [34]. Dealing with an analytic expression of the function, rather than a discrete group of points, e.g. by sampling the time evolution of AoI, allows for precise calculations of the statistical quantities, needed to aggregate the collected data for the analysis. The drawback is that those calculations might be not straightforward to implement. The statistical quantities taken into consideration are mean and median values. The formula applied to compute the exact value of the AoI in each instant is the following:

$$\Delta(t) = t - U(t) \quad (1)$$

where $\Delta(t)$ is the AoI at instant t , and $U(t)$ the generation time of the newest data received. This formula represents the time evolution of the AoI metric, which assumes the shape of an irregular sawtooth, rising linearly while waiting for new messages and suddenly falling to a lower value at the reception of a new message. The function is always positive, with a lower bound given by the one-way delay of the network. Each linear section has a 45° inclination, i.e. slope 1, so the distance covered on the x-axis is the same as the one on the y-axis for each segment. The function is integrable.

Mean Value. The mean value is the simplest form of data aggregation. However, dealing with a function requires a different approach than the simple arithmetic mean applicable for a discrete set of points. To compute the mean of the AoI function we used the integral mean, defined as the ratio between the definite integral of the function over the given interval and the length of the interval:

$$f : [a, b] \rightarrow \mathbb{R} \text{ bounded and integrable in } [a, b] \quad (2)$$

$$M(f, [a, b]) = \frac{1}{b-a} \int_a^b f(x) dx$$

In our case, the interval length is given by the time elapsed between the first and last message received by the subscriber.

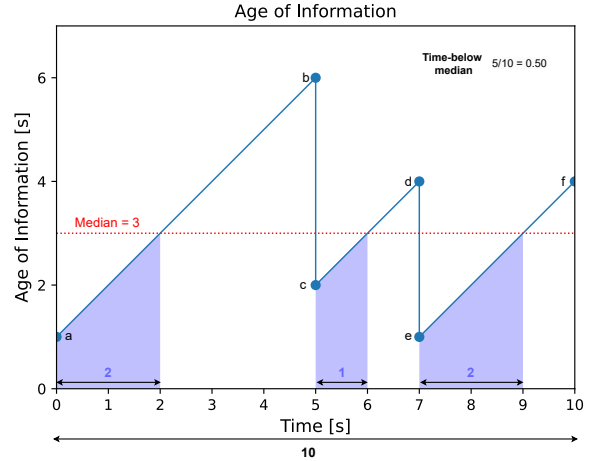


Fig. 2: Median definition for AoI function

Median Value. Besides the mean value, we compute the median value, which is known to be more robust to noise. The problem is to find an extension of the median applicable to a function and not to a discrete set of points, obtaining the same type of relationship that exists between the arithmetic mean and integral mean. The median is defined as the value separating the higher half from the lower half of the points in the set. The concept of half the points of the set can be extended to half the length of the interval over which the AoI function is defined. Based on this new definition, the median value can be assumed as the level of AoI for which the sum of the lengths of the intervals on the x-axis that have associated AoI less than (greater than) the median is exactly half of the total length of the interval over which the function is defined. The visualization of this definition is reported in Figure 2. To compute the median of a sawtooth function, we devised a method based on projecting the function segments on an axis. This method obtains the exact median value without involving complex computations. The exploited property is the unitary slope, which allows us to work on either the x-axis or the y-axis. The method is based on the projection of each segment on a vertical axis, referred to as the projection axis. The projections on the projection axis can generate overlapping regions. For each region, a weight is assigned, computed as the number of different projections that fall in it. Next, we compute a weighted sum as the length of each region times the associated weight. This sum will be referred to as the total extension. Finally, we iterate over the regions, bottom-up, computing their extension, i.e. their weighted length, and summing them up until half of the total extension is reached. The last sum will probably exceed half of the total extension, so only a fraction of the weighted length of the last region is to be considered. The point on which the iteration stops, i.e. the quote on the axis, corresponds to the median value. The construction of the projection axis is reported in Figure 3 and a possible implementation is shown in Algorithm 1.

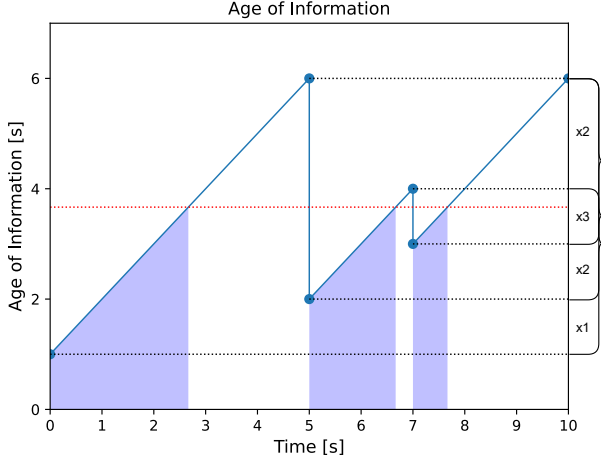


Fig. 3: Projection algorithm.

B. Energy

The Oti power monitor returns the total energy absorbed during the execution of the experiment. Given that the duration of an experiment is not fixed, as we will see in Section V, we normalized the measured energy over the experiment execution time. The result is the average power consumed by the device in the experiment.

C. Pareto Efficiency

The two metrics, AoI and energy, are considered together for the energy-constrained nature of IoT devices. This can introduce additional complexity in the analysis: the objective is to optimize both, but there is a trade-off to be resolved. The best method for presenting the results is to use a tool that shows all possible optimal solutions and leaves it up to the reader to determine which of those presented is the most suitable configuration for a given system. The tool that perfectly matches the above requirements is the Pareto front, built up by a set of Pareto efficiencies. Pareto efficiency is a concept introduced by the Italian economist and engineer Vilfredo Pareto that states that, given a set of resources an allocation is efficient if it is not possible to improve the condition of one individual without worsening those of another, i.e. Pareto improvements are not available. This concept can also be applied in multi-objective optimization when there is no feasible solution that minimizes all objective functions simultaneously [35]. Let us consider a set of points in the plane whose coordinates represent AoI and energy, respectively, each associated with a particular configuration. The Pareto efficient solutions are those for which one metric cannot be improved without worsening the other. The subset of Pareto efficient solutions represents the Pareto front on which a designer can choose the solution to adopt, considering possible constraints of the system in terms of AoI and energy. The choice can be considered as an a-posteriori assignment of weights to the metrics, based on the knowledge of the

Algorithm 1 Projection median

```

function COMPUTE_PROJECTION_MEDIAN(timestamps) ▷
Returns a float
    projections ← empty list
    extension ← 0
    for i ← 1 to len(timestamps) - 1 do
        start_aoi ← timestamps[i-1][“rx”] - timestamps[i-1][“gen”]
        end_aoi ← timestamps[i][“rx”] - timestamps[i-1][“gen”]
        projections.append((start_aoi, 1)) ▷ +1 marks the
begin of the projection
        projections.append((end_aoi, -1)) ▷ -1 marks the
end of the projection
        extension ← extension + (end_aoi - start_aoi)
    end for
    projections.sort(key ← x : x[0]) ▷ Sort list of tuples
using the second element as key
    weight ← 0
    curr_ext ← 0
    start ← -1
    for projection in projections do
        if start ≠ -1 then
            region ← projection[0] - start ▷ Region length
            if curr_ext + region × weight ≥ extension/2 then
                return start + (extension/2 - curr_ext)
            end if
            curr_ext ← curr_ext + region × weight
        end if
        weight ← weight + projection[1] ▷ Weight is
increased/decreased by 1
        start ← projection[0] ▷ Start of new region on
projection axis
    end for
end function

```

considered system. The points having both coordinates worse than other points are referred to as Pareto-dominated and the associated configuration doesn't provide an optimal choice for any system, thus they can be discarded. An example of the Pareto front is reported in Figure 4.

V. EXPERIMENTAL RESULTS

Our experiments aim to evaluate the combination of the two metrics of interest when varying different operation parameters. Specifically, we evaluated the impact on energy and AoI when varying: (i) the publisher generation rate, (ii) the additional delay between the publisher and the broker, i.e. the RPI and the server, (iii) the payload size of the publisher messages, (iv) the number of cores used on the RPI, (v) the transport protocol. The number of generated messages in one run is equal to the nominal generation rate multiplied by 60, which corresponds to a duration of 60 seconds. However, as we will highlight in the next sections, the real generation rate can be lower than the nominal rate. In these cases, the duration

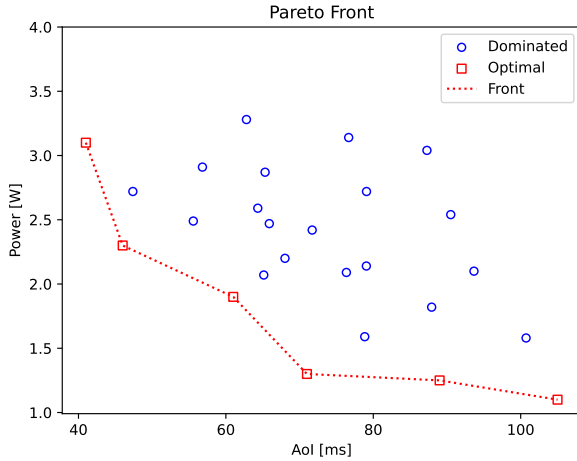


Fig. 4: Example of Pareto Front.

of an experiment will be longer. For each configuration, we executed one run, except for the last one, where we executed 30 runs. Besides the metrics used to compute energy and AoI, the RPI collects also context metrics useful to explain the obtained results, such as the cellular network quality and the clock synchronization precision.

A. Impact of the Generation Rate

For these experiments, we set the message payload to 128 B, no additional delay on the cellular link, and a single core on the RPI. We varied the nominal generation rate on the publisher from 1 msg/s to 8000 msg/s, with the following steps: 1, 10, 100, 1000, 2000, ..., 8000. We show results for both the transport protocols (QUIC and TLS), and all the buffering strategies. Figure 5a shows the relationship between the real generation rate and the nominal generation rate, for both transport protocols and the different buffering strategies. The figure shows that the buffer size poses an upper limit on the real generation rate. The bigger the buffer, the higher the real rate that can be obtained. For FIFO policies, this happens because, once the buffer is full, the publisher blocks. This automatically reduces the real publishing rate so that it is compatible with the maximum message throughput that can be sent out via the network. The presence of a larger buffer allows the publisher to cope with the transient reduction of throughput due to changing network conditions and, more importantly, it allows the aggregation of multiple messages within a single transport-layer packet. For the DROP buffering strategy, the real rate corresponds to the number of messages that are transmitted by the RPI. It has to be noted that for the FIFO 1 policy, the rate obtained by TLS is much higher than the one obtained by QUIC. This happens because in its base configuration, TCP with TLS uses the Nagle algorithm, which performs a much more aggressive aggregation than QUIC.

For each rate and each protocol/transport configuration, we computed median AoI and average power. The median AoI starts from high values when the rate is low, and then decreases

to around the nominal delay value when the rate is 2000 msg/s. Then, it starts increasing again for all FIFO configurations. For the DROP configurations, instead, it remains at the minimum value. This is expected, as the property of the DROP policy is to deliver always the most “fresh” message. Figure 5b, shows this trend for rates from 100 to 4000. It must be noted that the QUIC configurations obtain always lower AoI values than their corresponding TLS ones. Figure 5c shows the power consumption over the nominal rate. After this initial sudden increase, the power continues rising with the rate but with a slower slope. This trend is valid for all configurations up to the rate of 2000 msg/s. From such a rate onward the DROP policy stops increasing and the same applies for FIFO 1, but only in the QUIC configuration. The FIFO-1 TLS encounters an upper bound around the rate of 5000 msg/s. Other configurations, even if subjected to some fluctuations, present a quite evident increasing trend up to the maximum rate. This suggests that the power consumption is dominated by the transmission rate. Once the maximum rate for a configuration is reached, further increases in the nominal rate won’t produce any significant variation in the average power. It must be noted that below 2000 msg/s QUIC always shows a higher power consumption. Over that threshold, things get more confused, even if generally QUIC consumes more than its corresponding TLS configuration.

Figures 5d and 5e show the Pareto fronts for the FIFO policies and the DROP policies, respectively. The results for the rate of 1 msg/s are omitted for the sake of clarity, as they obtain a median AoI of approximately 500 ms, even if the power consumption is extremely low. For the FIFO configurations, the rates that appear in the front do not exceed 2000 msg/s. As previously observed, excessively high transmission rates do not guarantee advantages for either power consumption or AoI. Besides that, in general, the lower the rate the lower the consumption and the higher the AoI, and vice-versa, and the QUIC configurations obtain the lower AoI. It is worth noticing that the high density of points in the left extreme also shows that, once approaching the lower AoI bound, any further improvement requires a significant increment in the power consumption. In the DROP configurations, we can notice that also rates higher than 2000 msg/s are present in the front. This happens because higher rates, even if higher than the nominal one, produce “fresher” information, thus helping keep the AoI low, at the cost of possible information loss.

B. Impact of Additional Delay

For these experiments, we artificially applied additional delay on the cellular link in both directions (uplink and downlink). Specifically, the delay was added on the server machine via the Linux Traffic Control (TC) command. We performed runs with additional delays from 20 to 80 ms, at steps of 20 ms. For what concerns AoI, as could be expected, an upward shift can be appreciated in Figure 6, which shows the raw results for the QUIC, FIFO 16 configuration with a rate of 1000 msg/s. The shift is less evident for lower rates, as the AoI values are already high. The maximum achievable

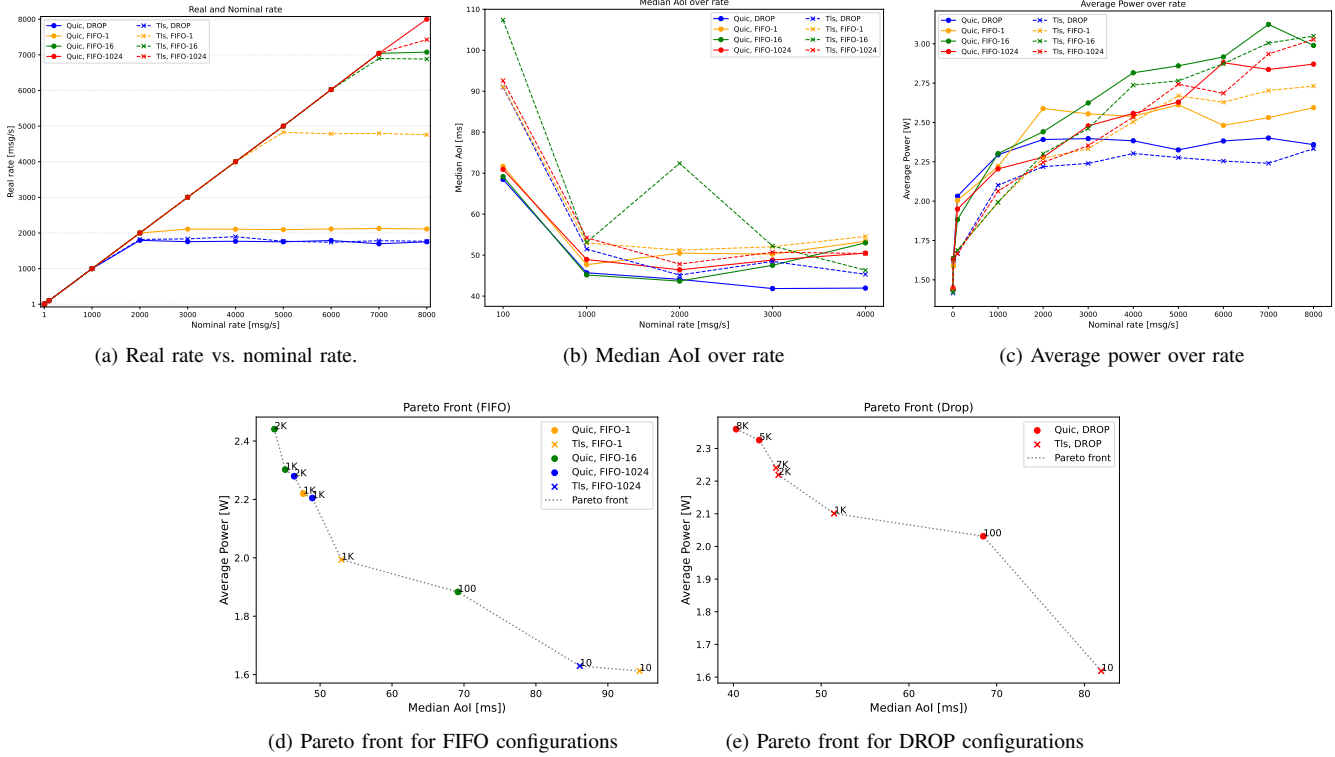


Fig. 5: Generation rate results.

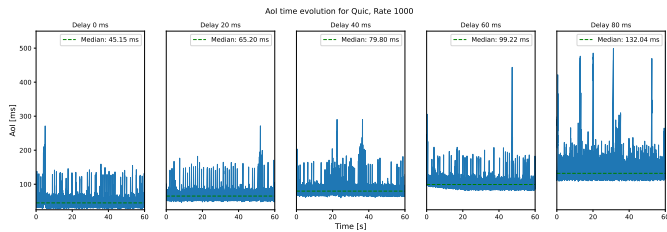


Fig. 6: AoI values for different additional delays.

rate is affected too. In general, a long queue allows higher rates, as already observed. However, for longer queues (namely FIFO 16 and FIFO 1024), by increasing the delay there is an overall reduction of the maximum rate, mainly for QUIC. The phenomenon can be visualized in Figure 7a, where, starting from a 40 ms additional delay, the rate achieved by QUIC is progressively lower than the one obtained by TLS. The causes for this behavior are beyond the scope of this work, however, they could lie at the intersection of the following aspects:

- **Congestion control.** The congestion control algorithm is the same, Cubic, for both transport protocols. However, the operational parameters may differ, resulting in different performance when varying the network delay.
- **Flow control.** The advanced flow control mechanism of QUIC based on multiple streams is not exploited by the implemented tool, so in this configuration also QUIC may suffer from the head-of-line blocking problem.

- **Aggregation.** The aggregation at the transport layer for TLS/TCP is based on the Nagle algorithm, that, for high transmission rates, allows for sending only fully sized segments, independently from the network delay, while QUIC adopts a blander aggregation mechanism.
- **Kernel optimization.** The Linux kernel on the RPI doesn't offer optimization for the UDP protocol, such as Generic Segmentation Offload (GSO), potentially reducing the performance of QUIC.

We conclude the analysis of the impact of the additional delay by showing the Pareto fronts for FIFO and DROP buffering strategies (Figures 7b and 7c, respectively). In the figures, for each additional delay (including no additional delay) a separate front is depicted. The leftmost front is the one with the minimum delay and the rightmost front is the one with the highest delay. For the FIFO configurations, the considerations for the case without additional delay apply also to the other cases, i.e. lower rates guarantee a low power consumption, at the cost of higher AoI, and vice-versa. In addition, QUIC configurations obtain lower AoI, while TLS ones obtain lower energy consumption, as already observed in the case with no additional delay. Rates higher than 2000 msg/s do not guarantee any benefits except in two cases. In both cases, these results are obtained with a FIFO 1 queue and the QUIC protocol. Considering that in the FIFO configurations, the generation rate adapts to the transmission rate, the result is to be considered equal to one obtained by a lower rate.

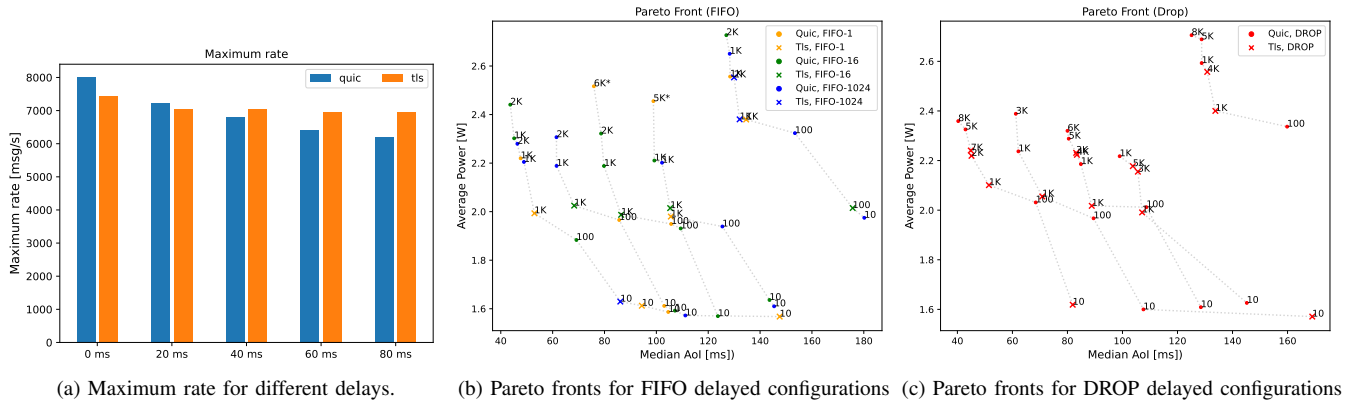


Fig. 7: Additional delay results.

TABLE III: Median AoI varying the payload size for TLS, FIFO-16, rate 100 configuration

Payload size	Median AoI
128B	107.38
256B	85.04
512B	65.52
1KB	60.24
2KB	55.46

The improvement in terms of AoI with respect to the second highest point in the front is negligible, at the unjustifiable cost of higher energy consumption. The same considerations found for the case with no additional delay apply also to the DROP configurations. In particular, these configurations benefit also from higher rates, as already pointed out.

C. Impact of Different Payload Sizes

In previous experiments, we considered a fixed payload size of 128 B. However, there could be scenarios characterized by advanced sensors producing more complex, thus bigger data structures. In addition, multiple sensors could be attached to the same device which would in turn produce bigger packets containing more than one message. In these experiments, we evaluate the impact of greater payload sizes on energy consumption and AoI. We consider the following payload sizes: 128 B, 256 B, 512 B, 1024 B, 2048 B. The maximum payload size of 2048 B allows us to consider application scenarios where a large amount of data has to be fitted in a single message, as well as to account for possible effects on the AoI of messages that do not fit in a single segment at the transport layer. For these experiments, we considered only rates up to 1000 msg/s as (i) the best results for AoI in the previous experiments were obtained with rates around 1000-2000 msg/s, (ii) the combination of large payload size and high transmission rate would produce a very high throughput which could not be sustainable by the RPI and IoT devices in general. The analysis of the Pareto fronts highlights a slightly higher

power consumption for the configurations with higher payload sizes, while the AoI decreases as the payload increases, for the rate of 100 msg/s and in some configurations even 1000 msg/s. Table III shows this behavior for the TLS, FIFO 16, rate 100 msg/s configuration. Particularly interesting are the Pareto fronts for the payload size of 2048 B (Figure 8), which show the configurations with a rate of 100 msg/s as the best ones for AoI. In fact, at higher rates, the AoI values are extremely high. This happens because the system is not able to handle the required throughput, and this does not depend on the queue size, as testified by Figure 9, which shows the anomalous behavior for both the FIFO 1024 and the DROP queues. Therefore, the cause seems to be due to oversized buffering that takes place somewhere between the transmitter and the receiver, either in the RPI (on-device bufferbloat [36]) or in the cellular network infrastructure. It has to be noticed a difference between the AoI obtained with QUIC and TLS, with QUIC that always obtains a better performance. For what concerns power consumption, the least power-demanding transmission protocol is TLS, however, when the payload size increases the difference between the protocols tends to shrink, especially for the FIFO configurations.

D. Impact of Multiple Cores

In this experiment, we evaluate the impact on power consumption and AoI of enabling an additional core on the RPI. The software we developed is single-threaded, and concurrency is implemented via asynchronous mechanisms, that exploit the idle times dictated by I/O operations to carry out other tasks. However, in parallel with our software, multiple kernel threads are executed, responsible for handling network operations and other system tasks. Thus, enabling more than one core could benefit the overall system's performance.

Enabling the second core allowed the system to reach higher rates, and, more importantly, a lower AoI. This is particularly evident for QUIC in the FIFO 1 configurations, as can be observed in Figure 10a. This effect is not found in the DROP configurations, as the possibility to overwrite the buffer content allows always to deliver the “freshest” information.

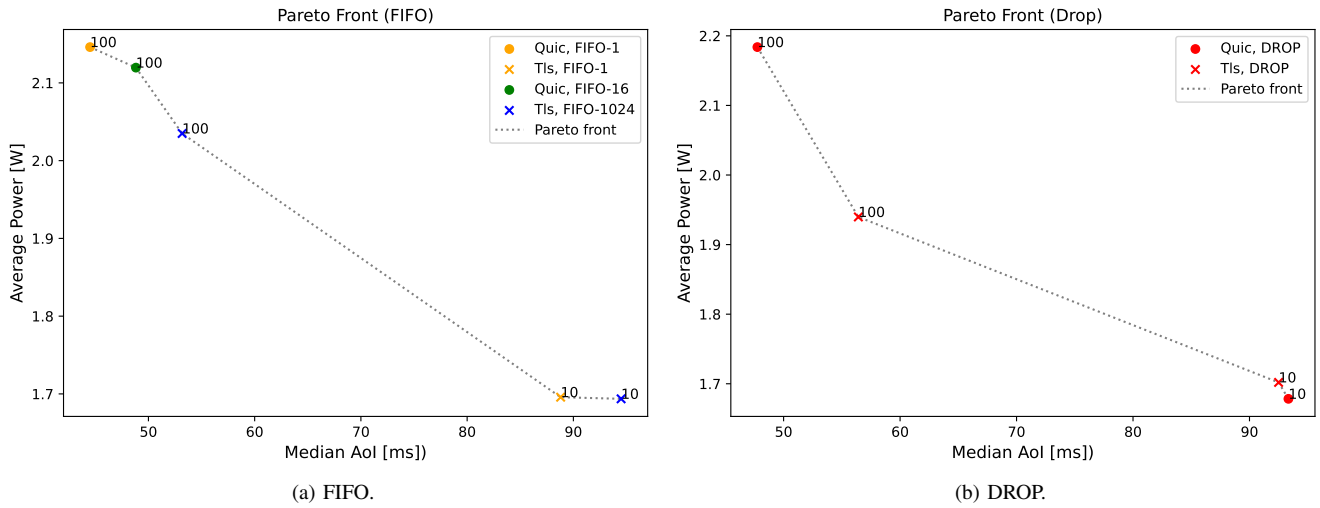


Fig. 8: Pareto fronts for 2048 B payload configurations.

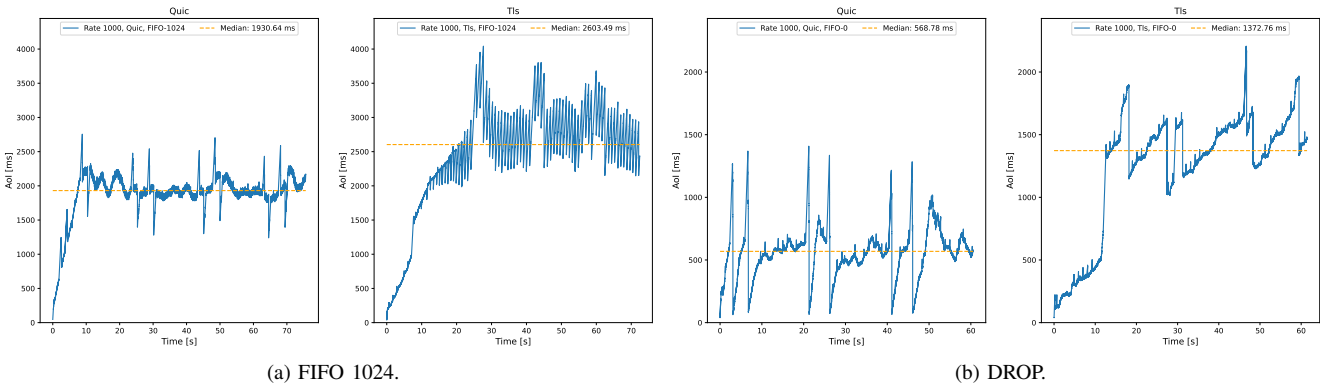


Fig. 9: Time evolution for 2048 B payload, rate 1000 msg/s.

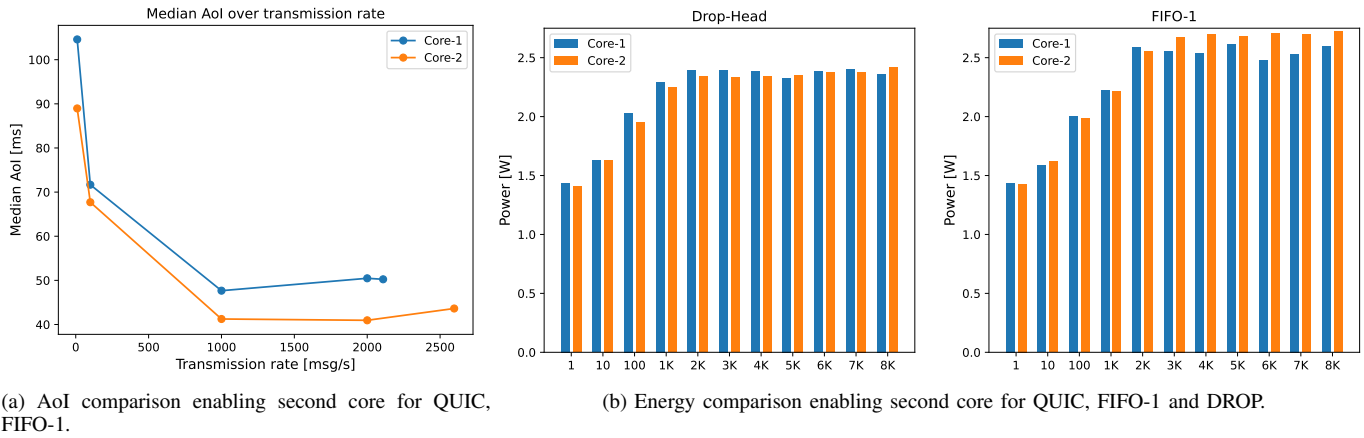
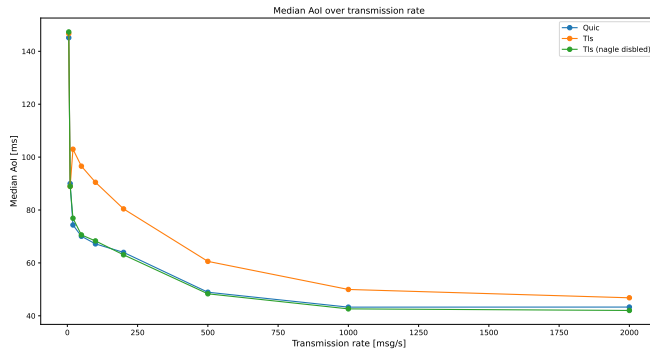


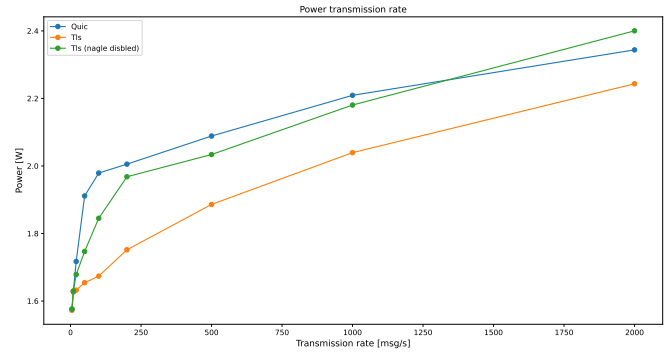
Fig. 10: Results for multiple cores configurations.

The positive impact of the second core has a drawback, paid in terms of additional energy required to power the hardware component, but not in all configurations, as shown

in Figure 10b. For DROP configurations, it is not possible to spot a clear difference in power consumption. For FIFO configurations instead, the impact on the power consumption



(a) AoI over transmission rate.



(b) Power over transmission rate.

Fig. 11: Impact of the transport protocol for FIFO 16 configurations.

is significant as the rate gets higher. This is because the second core allows higher transmission rates, which, in turn, can increase the power consumption of the network card.

E. Impact of the Transport Protocol

We finally executed a set of experiments aimed at quantifying the impact of the transport protocol on power consumption and AoI. We considered three transport protocols: QUIC, TLS, and TLS with Nagle’s algorithm disabled. We added the latter because, as aforementioned, the aggregation plays a crucial role in the maximum achievable rate and the AoI, often resulting in a discriminant factor between QUIC and TLS. We considered just two buffering policies: FIFO 16 and DROP. We used just a single core and a fixed payload size of 128 B. We limited the maximum generation rate to 2000 msg/s but we explored more values in the range of generation rates, in particular: 5, 10, 20, 50, 100, 200, 500, 1000, 2000. No additional delays were considered. Finally, we kept the duration of a single experiment to 60 s, but we repeated each run 30 times. This is to ensure statistical robustness. We aggregated the results (power consumption and AoI) of each repetition of the same setup by taking the median value. The results for the two buffering strategies are extremely similar, thus, to avoid confusion, we show just the ones for FIFO 16.

Figure 11a shows the AoI obtained when varying the transmission rate. The better performance in terms of AoI of QUIC with respect to standard TLS is confirmed. However, the most interesting result is that, by disabling Nagle’s algorithm, TLS yields the same if not slightly better results as QUIC. This result shows that the main difference in terms of AoI between the transport protocols is given by the aggregation mechanism at the transport layer, much more aggressive when Nagle’s algorithm is enabled. Standard TLS shows a peculiar trend for rates higher than 10 msg/s. AoI suddenly and unexpectedly increases for a 20 msg/s rate, to start decreasing again afterward, but assessing of significantly higher values than the other two protocols. This is due to Nagle’s algorithm, which is triggered by acknowledgments: when the transmission rate produces messages with a period higher than the network RTT (which we recall is ~ 80 ms between the publisher and the

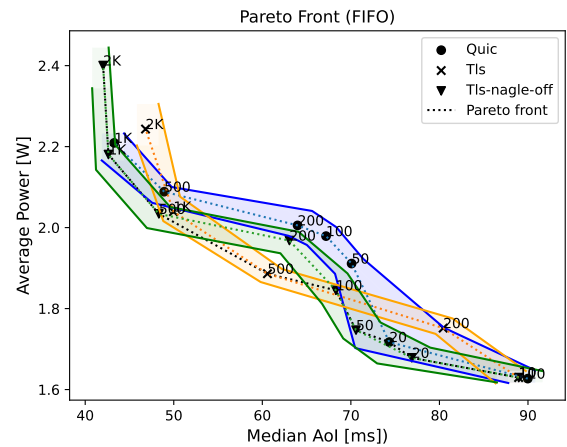


Fig. 12: Pareto fronts for FIFO configurations.

broker), Nagle’s algorithm delays transmission until acks are received or the segment gets full, and this negatively affects AoI despite the increase of the transmission rate.

The AoI improvement obtained by removing the aggregation has a consequence from the energy point of view, as shown in Figure 11b. The TLS curve with Nagle’s algorithm disabled is much closer to the QUIC curve than the standard TLS curve. The QUIC configuration seems to be the most energy-demanding, at least up to the highest considered rate, for which the curves swap. The lack of aggregation in the TLS with Nagle’s algorithm disabled may cause the inversion. The QUIC protocol is responsible for lighter aggregation than Nagle’s algorithm, so the effects on the AoI are limited, but when the transmission rate increases, having some messages shipped in the same transport layer packet allows for fewer transmissions and therefore less energy spent. A simple analysis of traces collected for a rate of 2000 msg/s shows a mild aggregation for QUIC, around 2 messages per segment, while TLS without Nagle’s algorithm doesn’t provide any form of aggregation.

Figure 12 shows the Pareto fronts for the three considered protocols. Besides the median values, the 25th and 75th

percentiles for both AoI and power are also reported, which identify three bands around the Pareto front of each protocol. A larger band means a greater variability of data and thus less confidence in the single point obtained via aggregation. When the bands are far enough it is quite safe to state that one solution is better than the other, however, if the bands intersect each other, the two solutions are almost equivalent, thus the choice should be taken considering other aspects. The Pareto front identified by the combination of the three fronts is finally depicted as a black dotted line.

In the right part of the graph, the three transport protocols behave similarly, as highlighted by the three overlapped bands. Moving towards the left, TLS dominates the other protocols, leaving a space from one band to the others and having the Pareto front completely in its band. Keeping moving in the same direction the standard TLS is no longer able to guarantee the optimal results, so it is replaced by the other two protocols, for which there isn't a clear winner. It is worth noticing that QUIC presents a larger variability, indicated by a larger band, especially for slower rates, i.e. on the right part of the graphs, while both versions of TLS generate a narrower band. Moreover, the Pareto fronts show that the aggregation of Nagle's algorithm can save energy, at the cost of a higher AoI. The result is that for a middle region, where the AoI is not minimized, the standard TLS seems to guarantee the best trade-off. When the requirements on AoI are the most stringent, the aggregation limits the performance, thus disabling Nagle's algorithm or adopting QUIC could help to meet the requirements. The simple fine-tuning of the TLS protocol, derived from the underlying TCP option, can guarantee optimal protocol results even in those scenarios where QUIC seemed to provide better results, so in many cases the greater availability of TLS may favor this protocol over the emerging QUIC, for which the standardization process and availability are not yet comparable to the classic TLS over TCP.

VI. CONCLUSION

In this work, we conducted a combined study of AoI and energy consumption in an IoT environment based on MQTT, where a battery-operated device acts as a data publisher. Experimental results show that improving the AoI requires to increase the energy expenditure, as both of them depend somehow on the transmission rate. However, our contributions are not limited to this result. We considered a wide range of system operational parameters and showed their impact on both AoI and energy. Our results provide system designers with guidelines and numbers useful for finding the desired trade-off between AoI and energy consumption, according to the system requirements.

Thanks to Pareto fronts, we highlighted all the optimal solutions, leaving to the final designer the possibility to choose which operational point better satisfies the specific system requirements. The results showed that a DROP buffering policy is better for the application queue management, but paying the cost of message loss which may not be admitted in

some scenarios. Therefore, FIFO buffering strategies should be considered as well, especially when employing long queues, that allow for aggregation at the transport level resulting in a dramatic improvement in terms of reachable throughput. The aggregation at the transport layer was revealed to be a paramount factor to take into consideration. The aggressive aggregation enforced by Nagle's algorithm is the main factor causing different results for the two transport protocols, TLS and QUIC. QUIC able to guarantee a better AoI than standard TLS at the cost of higher energy consumption, at least for the rates employs in the analysis. This difference disappears when disabling Nagle's algorithm, making the two protocols comparable.

Overall, our study confirmed the possibility of adopting QUIC as a reliable transport protocol, replacing TCP. However, the immaturity of the new protocol may represent an obstacle to its adoption, favoring a more standardized protocol for which compatibility and support are much larger.

ACKNOWLEDGMENT

REFERENCES

- [1] Q. Abbas, S. A. Hassan, H. K. Qureshi, K. Dev, and H. Jung, "A comprehensive survey on age of information in massive IoT networks," *Comput. Commun.*, vol. 197, pp. 199–213, 2023.
- [2] S. Kaul, R. Yates, and M. Gruteser, "Real-time status: How often should one update?" in *Proc. IEEE INFOCOM '12*, 2012, pp. 2731–2735.
- [3] M. Patra, A. Sengupta, and C. S. R. Murthy, "On minimizing the system information age in vehicular ad-hoc networks via efficient scheduling and piggybacking," *Wirel. Netw.*, vol. 22, pp. 1625–1639, 2016.
- [4] N. Suma, S. R. Samson, S. Saranya, G. Shanmugapriya, and R. Subhashri, "IoT based smart agriculture monitoring system," *Int. J. Recent Innov. Trends Comput. Commun.*, vol. 5, no. 2, pp. 177–181, 2017.
- [5] C. Chaccour and W. Saad, "On the Ruin of Age of Information in Augmented Reality over Wireless Terahertz (THz) Networks," in *Proc. of GLOBECOM '20*, 2020, pp. 1–6.
- [6] C. Caiazza, V. Luconi, and A. Vecchio, "Saving energy on smartphones through edge computing: an experimental evaluation," in *Proc. of ACM SIGCOMM NET4us '22*, 2022, p. 20–25.
- [7] C. Caiazza, S. Giordano, V. Luconi, and A. Vecchio, "Edge computing vs centralized cloud: Impact of communication latency on the energy consumption of LTE terminal nodes," *Comput. Commun.*, vol. 194, pp. 213–225, 2022.
- [8] C. Caiazza, V. Luconi, and A. Vecchio, "Measuring the Energy of Smartphone Communications in the Edge-Cloud Continuum: Approaches, Challenges, and a Case Study," *IEEE Internet Comput.*, vol. 27, no. 6, pp. 29–35, 2023.
- [9] —, "Energy consumption of smartphones and IoT devices when using different versions of the HTTP protocol," *Pervasive Mob. Comput.*, vol. 97, p. 101871, 2024.
- [10] V. Tripathi and S. Moharir, "Age of information in multi-source systems," in *Proc. of GLOBECOM '17*, 2017, pp. 1–6.
- [11] A. Valehi and A. Razi, "Maximizing Energy Efficiency of Cognitive Wireless Sensor Networks With Constrained Age of Information," *IEEE Trans. Cogn. Commun. Netw.*, vol. 3, no. 4, pp. 643–654, 2017.
- [12] H. B. Beytur, S. Baghaee, and E. Uysal, "Towards aoi-aware smart iot systems," in *Proc. of ICNC '20*, 2020, pp. 353–357.
- [13] I. Kadota, M. S. Rahman, and E. Modiano, "WiFresh: Age-of-Information from Theory to Implementation," in *Proc. of ICCCN '21*, 2021, pp. 1–11.
- [14] L. Eggert, "Towards Securing the Internet of Things with QUIC," 2020.
- [15] J. Dizdarević and A. Jukan, "Experimental Benchmarking of HTTP/QUIC Protocol in IoT Cloud/Edge Continuum," in *Proc. of IEEE ICC '21*, 2021, pp. 1–6.
- [16] A. Alqattaa, D. Loebenberger, and L. Moeges, "Analyzing the Latency of QUIC over an IoT Gateway," in *Proc. of IEEE COINS '22*, 2022, pp. 1–6.

- [17] S. Jeddou, F. Fernández, L. Diez, A. Baina, N. Abdallah, and R. Agüero, "Delay and Energy Consumption of MQTT over QUIC: An Empirical Characterization Using Commercial-Off-The-Shelf Devices," *Sensors*, vol. 22, no. 10, 2022.
- [18] S. Kaul, M. Gruteser, V. Rai, and J. Kenney, "Minimizing age of information in vehicular networks," in *Proc. of IEEE SAHCN '11*, 2011, pp. 350–358.
- [19] R. D. Yates and S. Kaul, "Real-time status updating: Multiple sources," in *Proc. of IEEE ISIT '12*, 2012, pp. 2666–2670.
- [20] Y. Inoue, "Analysis of the Age of Information with Packet Deadline and Infinite Buffer Capacity," in *Proc. of IEEE ISIT '12*, 2018, pp. 2639–2643.
- [21] F. Chiariotti, A. A. Deshpande, M. Giordani, K. Antonakoglou, T. Mahmoodi, and A. Zanella, "QUIC-EST: A QUIC-Enabled Scheduling and Transmission Scheme to Maximize Vol with Correlated Data Flows," *IEEE Commun. Mag.*, vol. 59, no. 4, pp. 30–36, 2021.
- [22] Y. Gu, H. Chen, Y. Zhou, Y. Li, and B. Vucetic, "Timely Status Update in Internet of Things Monitoring Systems: An Age-Energy Tradeoff," *IEEE Internet Things J.*, vol. 6, no. 3, pp. 5324–5335, 2019.
- [23] K. Saurav and R. Vaze, "Online Energy Minimization Under a Peak Age of Information Constraint," *IEEE J. Sel. Areas Inf. Theory*, vol. 4, pp. 579–590, 2023.
- [24] B. T. Bacinoglu, Y. Sun, E. Uysal-Bivikoglu, and V. Mutlu, "Achieving the Age-Energy Tradeoff with a Finite-Battery Energy Harvesting Source," in *Proc. of IEEE ISIT '18*, 2018, pp. 876–880.
- [25] J. Huang, H. Gao, S. Wan, and Y. Chen, "AoI-aware energy control and computation offloading for industrial IoT," *Future Gener. Comput. Syst.*, vol. 139, pp. 29–37, 2023.
- [26] C. Sönmez, S. Baghaee, A. Ergişi, and E. Uysal-Biyikoglu, "Age-of-Information in Practice: Status Age Measured Over TCP/IP Connections Through WiFi, Ethernet and LTE," in *Proc. of IEEE BlackSeaCom '18*, 2018, pp. 1–5.
- [27] WaveShare, "SIM8200EA-M2 5G HAT," https://www.waveshare.com/wiki/SIM8200EA-M2_5G_HAT, accessed: April 4, 2024.
- [28] Qoitech, "Oti Arc Pro by Qoitech," <https://www.qoitech.com/otii-arc-pro/>, Qoitech AB, accessed on February 21, 2024.
- [29] Dirkjan Ochtman and Benjamin Saunders and Jean-Christophe Begue, "quinn: A Rust implementation of the QUIC transport protocol," <https://quinn-rs.github.io/quinn>, accessed on February 21, 2024.
- [30] Tokio Developers, "Tokio: A runtime for writing reliable asynchronous applications with Rust," <https://tokio.rs/>.
- [31] Rustls Developers, "rustls: A modern TLS library in Rust," <https://github.com/rustls/rustls>.
- [32] Bytebeamio and contributors, "mqttbytes: MQTT packet encoder/decoder in Rust," <https://github.com/bytebeamio/mqttbytes>.
- [33] Eclipse Foundation, "Eclipse Paho MQTT Client," <https://eclipse.dev/paho/>, accessed on February 21, 2024.
- [34] R. D. Yates, Y. Sun, D. R. Brown, S. K. Kaul, E. Modiano, and S. Ulukus, "Age of information: An introduction and survey," *IEEE J. Sel. Areas Commun.*, vol. 39, no. 5, pp. 1183–1210, 2021.
- [35] P. Ngatchou, A. Zarei, and A. El-Sharkawi, "Pareto Multi Objective Optimization," in *Proc. of ISAP '05*, 2005, pp. 84–91.
- [36] Y. Guo, F. Qian, Q. A. Chen, Z. M. Mao, and S. Sen, "Understanding On-device Bufferbloat for Cellular Upload," in *Proc. of ACM SIGCOMM IMC '16*, 2016, p. 303–317.